



Fluorescence characterization of chemical microenvironments in hydrophobically modified chitosan

Georgianna L. Martin^a, Justin A. Ross^b, Shelley D. Minteer^c, David M. Jameson^{b,*},
Michael J. Cooney^{a,*}

^aHawaii Natural Energy Institute, University of Hawaii, Honolulu, HI 96822, USA

^bJohn Burns Medical School, University of Hawaii, Honolulu, HI 96822, USA

^cDepartment of Chemistry, St. Louis University, St. Louis, MO 63103, USA

ARTICLE INFO

Article history:

Received 16 July 2008

Received in revised form 4 February 2009

Accepted 17 February 2009

Available online 3 March 2009

Keywords:

Chitosan polymer

Fluorescence

Amphiphilic micelle

Chemical microenvironments

ABSTRACT

In this work we use the steady state and time-resolved fluorescence of free and enzyme-bound fluorophores to characterize the binding capacity of both unmodified and hydrophobically modified chitosan polymers. Additionally, fluorescence emission is used to qualitatively characterize the extent to which hydrophobic modification of the chitosan polymer affects the relative polarity of the resultant amphiphilic micelles. In total, these results are used to describe how fluorescence techniques can be used to characterize the chemical microenvironment provided by immobilization polymers such as chitosan. Commentary is also given on how this information can be correlated to enzyme activity and spatial distribution during the immobilization processes.

© 2009 Elsevier Ltd. All rights reserved.

1. Introduction

Within the context of biosensor and bio-fuel cell development, enzyme immobilization is used to achieve several important goals: (1) to extend active enzyme lifetime, (2) to both increase and maintain enzyme activity, (3) to avoid catalyst loss in flow systems, and (4) to increase enzyme loading. Of the immobilization techniques available, physical adsorption, entrapment, or encapsulation within polymers are often used because of their ability to retain enzyme without the loss of activity that can be associated with covalent attachment strategies. Selecting the best enzyme immobilization material requires careful matching of the material's chemical and physical properties with the enzyme of choice (Klotzbach, Watt, Ansari, & Minteer, 2008). Often the effects of a polymer's chemical properties, both before and after the immobilization process, are assumed without quantitative verification. This can lead to inaccuracies when correlating the polymer's material properties to enzyme activity and stability. Previously we have used fluorescence microscopy to demonstrate the spatial distribution of alcohol dehydrogenase within drop casted and air dried films. The findings suggest that this distribution could be correlated to the charge interaction between the enzyme and the poly-

mer (Konash, Cooney, Liaw, & Jameson, 2006). Recently we have also published a study on the spatial distribution of labeled enzyme immobilized within chitosan polymers of varying degree of hydrophobic modification (Martin, Minteer, & Cooney, 2009). In this work, we extend fluorescence techniques to characterize the chemical microenvironments of two immobilization polymers. These measurements are provided in terms of the polymer's binding capacity as provided by electrostatic and/or hydrophobic interactions, as well as the relative degree of polarity. While the biopolymer chitosan is presented as the model system, some data is also provided on Eastman AQ55, a water dispersible poly(ester sulfonic acid) anionomer, for comparative analysis.

Chitosan is a polycationic polysaccharide that is increasingly used to immobilize enzymes (Krajewska, 2004). Besides its biocompatibility, abundance and low cost, the presence of a repeating amine group along the polymer's backbone (Fig. 1) make it an attractive material for chemical modification. For example, Minteer's group has proposed the introduction of hydrophobic alkyl side chains (of varying carbon chain length) along the hydrophilic chitosan backbone to enhance the polymer's capacity to form amphiphilic micelles that can both retain enzyme and stabilize its activity (Klotzbach, Watt, Ansari, & Minteer, 2006). Although they have achieved some success, in some cases retaining activity for up to 60–70 days, they have also reported significant variation in enzyme activity as a function of side chain length (Klotzbach et al., 2008). This work addresses whether these variations can be explained in terms of differences in the chemical microenviron-

* Corresponding authors. Tel.: +1 808 956 7337; fax: +1 808 956 2336 (M.J. Cooney).

E-mail addresses: djameson@hawaii.edu (D.M. Jameson), mcooney@hawaii.edu (M.J. Cooney).

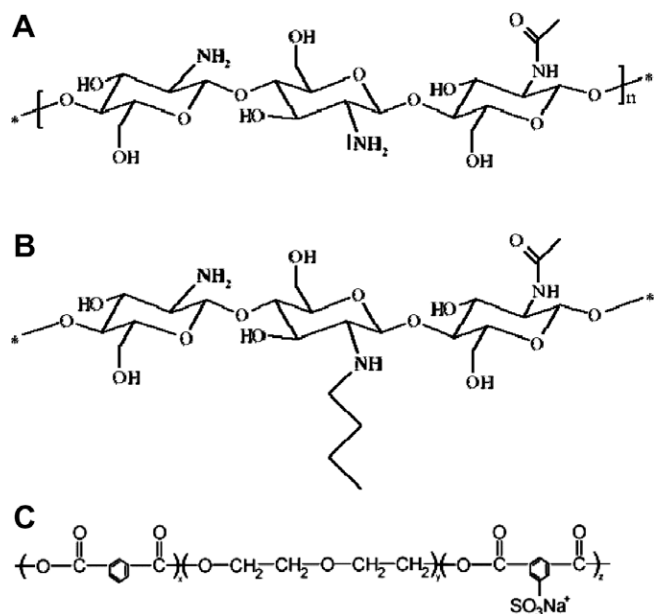


Fig. 1. Schematics of (A) Chitosan, (B) Butyl modified Chitosan, and (C) Eastman AQ55.

ment provided by the resultant amphiphilic micelles. Our results suggest that both the binding capacity and polarity are modified with alkyl chain length. However, the incorporation of the enzymes into chitosan's micellar structure does not occur in free solution. These results suggest that fluorescent spectroscopy and microscopy are useful tools to more accurately characterize the nature and dynamics of an enzyme's interactions with its immobilization matrix, and to correlate this interaction to activity of immobilized enzyme.

2. Materials and methods

2.1. Materials

Medium molecular weight (MMW ~ 250 kDa, internal measurement, data not shown) chitosan was purchased from Sigma-Aldrich (Sigma-Aldrich, St. Louis, MO). Eastman AQ 55 (MW = 7–8 kDa, Eastman publication CB-41A), a poly(ester sulfonic acid) anionomer, was obtained from Eastman Chemical Company, USA (Eastman Chemical Company, USA (<http://www.eastman.com>)). Alcohol dehydrogenase from baker's yeast was obtained from Sigma-Aldrich and used without further purification. Fluorescein sodium salt (95%) and the Nile Red were purchased from Sigma-Aldrich. Dansyl-chloride was purchased from Molecular Probes (Invitrogen Corporation, Carlsbad, California). The Rhodamine 123 (Rh 123) and 1-anilino-8-naphthalene sulfonate (ANS) was purchased from Invitrogen, Inc. The chemical structures of these probes can be seen in Fig. 2.

2.2. Polymer preparation

Medium molecular weight chitosan was first purified of residual fluorescent contaminants by rinsing 1 g aliquots over vacuum filtration with 500 mL of 0.5 M NaOH followed by 500 mL of HPLC grade methanol. The powder was then dried *in vacuo* at 25 mbar and 40 °C for 24 h. Aqueous solutions of 1 wt% medium molecular weight chitosan was prepared by dissolving 1 g of chitosan powder in 100 ml of 0.2 M acetic acid, yielding a final polymer concentration of (40 μM, pH 2.5). The butyl and octyl-modified chitosan was

prepared according to the method described in Klotzbach et al. (2006). Specifically, 0.5 g of medium molecular weight chitosan was dissolved in 15 ml of 1% acetic acid solution under rapid stirring until a viscous gel-like solution was achieved. 15 ml of methanol was then added and mixing allowed for an additional 15 min at which time 20 ml of butyraldehyde or octyraldehyde was added, followed immediately by addition of 1.25 g of sodium cyanoborohydride. The gel-like solution was continuously stirred until the suspension cooled to room temperature. The resulting product was separated by vacuum filtration and washed with 150 ml increments of methanol. The hydrophobically modified chitosan was then dried in a vacuum oven at 40 °C for 2 h, leaving a flaky white solid absent of any residual smell of aldehyde. A portion of this polymer was then suspended in 0.2 M acetic acid and vortexed for 1 h in the presence of 2 and 5 mm diameter yttria stabilized zirconia oxide beads (Norstone, Wyncote, PA) to create a 1 wt% solution. The resultant degree of modification is approximately 1% (internal NMR, Cooney, Petermann, Lau, & Minteer, 2009). Eastman AQ55 polymer was dissolved in ultra-pure water to a final volume ratio of 10% w/v (13 mM) and then diluted to 1%w/v in phosphate buffer (20 mM, pH 7).

2.3. Enzyme labeling

10 mg of yeast alcohol dehydrogenase (YADH) was dissolved in 1 mL of sodium bicarbonate buffer (20 mM, pH 8.5) yielding a final enzyme concentration of 70 μM. To this solution 47.5 μL of 4.0 mM 2,5-dansyl-chloride solution (freshly prepared in DMF) was added, resulting in an excess 10:1 dye to enzyme molar ratio. This solution was then incubated at room temperature for 1.25 h with stirring. The labeled enzyme was then purified by passing the solution over a PD10 size exclusion column previously rinsed and equilibrated with 50 mM TRIS buffer solution (pH 7). The fractions containing labeled enzyme were then pooled and dialyzed (MWCO 15000) against TRIS buffer (50 mM, pH 7) for 24 h at 4 °C. Dialysis was repeated against fresh solutions of TRIS buffer until no further change in the steady state fluorescence polarization of the enzyme containing fraction was measured. The final dye to molar enzyme ratio was measured at 3:1.

2.4. Fluorescence polarization

2.4.1. Steady state polarization

Steady state fluorescent polarization (P) is one of several fluorescent measurements that can be used to yield information regarding the capacity of a polymer's chemical microenvironment to interact with fluorophore molecules. Polarization, as defined by Perrin (Perrin, 1925a, 1925b, 1926; Weber, 1952a, 1952b), is

$$\left(\frac{1}{P} - \frac{1}{3}\right) = \left(\frac{1}{P_0} - \frac{1}{3}\right) \left(1 + \frac{3\tau}{\rho}\right) \quad (1)$$

The variables are defined as follows: fluorescence lifetime, or the time in which the number of excited molecules has dropped to 1/e of the original excited population, τ , the Debye rotational relaxation time, or the time at which the original orientation of the fluorophore has rotated through 68.42 degrees (the arccos of 1/e), ρ , and the limiting polarization or the polarization in the absence of rotation, P_0 . Perrin's equation suggests that a freely suspended fluorophore in buffer solution will have a characteristic rotational rate associated with its lifetime τ and rotational relaxation time ρ . Combined, P_0 , τ , and ρ define the limits to the measured polarization. The binding constant between the polymer and the fluorophore (i.e., the polymer concentration at which the steady state fluorescent anisotropy (equal to $2P/(3P)$) has reached 50% of its maximum value) can be measured by titrating the fluo-

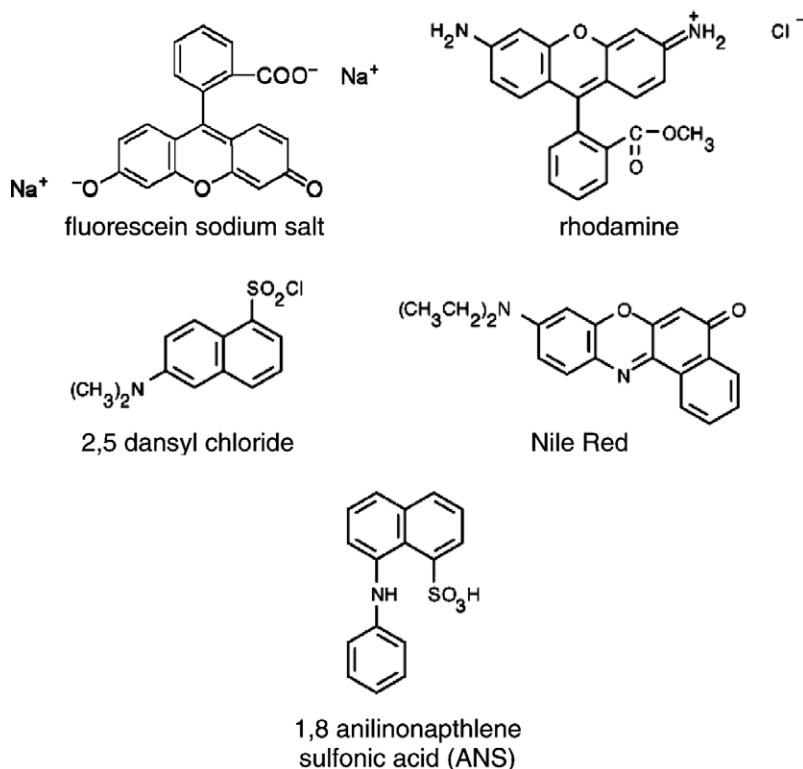


Fig. 2. Structure of fluorophores used in this work.

rophore containing solution with the polymer of interest and recording, the change in the steady state fluorescent polarization between these two limits (assuming that the quantum yield of the fluorophore is the same in the free and bound state).

The steady state polarization measurements were executed as follows. A stock solution of fluorescein sodium salt was dissolved in pH 7, 20 mM phosphate buffer and its concentration determined by measuring the optical density of the solution with a UV spectrophotometer, using an ϵ .c. of $81,000 \text{ cm}^{-1} \text{ M}^{-1}$ ($\lambda_{\text{max}} = 490 \text{ nm}$). Lower concentrations were then prepared in pH 4 and 6, 20 mM acetate buffer to be used in the polarization. Similarly, Rh 123 was dissolved in pH 8.0, 20 mM sodium bicarbonate buffer and the concentration determined by measuring the optical density of the solution with a UV spectrophotometer, using an ϵ .c. of $101,000 \text{ cm}^{-1} \text{ M}^{-1}$ ($\lambda_{\text{max}} = 530 \text{ nm}$). Lower concentrations were then prepared in pH 4 and 6, 20 mM acetate buffer and pH 6, 8, and 10, 20 mM phosphate buffers to be used in the polarization measurements. The steady state fluorescence polarization was measured using an ISS PC1 spectrofluorimeter (ISS, Champaign, IL). All fluorescein and Rh 123 measurements were performed using an excitation wavelength of 471 nm and a 500 nm long pass emission filter.

For the titration experiments, the molar ratios were calculated using the assumed molecular weights of each polymer, and the concentrations of the fluorophore and polymer solutions which were initially made on mass per unit volume basis.

2.4.2. Time-resolved polarization

Time-resolved polarization and excited state lifetime measurements were made on the labeled enzyme dissolved in acetate buffer (pH 3.5, 20 mM), unmodified and butyl-modified chitosan solutions (40 μM in 0.5 M acetic acid) using a time-resolved spectrofluorometer (ISS Chronos[®], Champaign, IL). The dynamic polarization was measured as a function of frequency and the associated lifetimes and rotational relaxation times were calculated using fluorescence modeling software, *Globals for Spectroscopy* (Gratton,

2006). A detailed description of these measurements can be found in (Jameson & Hazzlett, 1991). All dansyl-chloride YADH measurements were performed using an excitation wavelength of 375 nm and a 400 nm long pass emission filter.

2.5. ANS – Polymer measurements

ANS – polymer measurements were obtained by adding 50 μL of 50 mM ANS dissolved in DI water to separate 1 mL solutions of acetic acid (0.2 M), sodium bicarbonate buffer (20 mM, pH 8), 1 wt% unmodified chitosan in 0.2 M acetic acid, 1 wt% butyl-modified chitosan in 0.2 M acetic acid, 1 wt% octal-modified chitosan in 0.2 M acetic acid. The corrected emission spectra of each solution was measured from 400–700 nm using an ISS PC1 Photon Counting Spectrofluorometer (ISS, Champaign, IL) under identical conditions ($\lambda_{\text{exc}} = 375 \text{ nm}$, 1.0 mm slits).

2.6. Nile Red – Polymer measurements

The polymer scaffolds used in the Nile Red polymer measurements were prepared using a modification of the technique transferred to our lab (P. Atanassov, personal discussions) and reported in Yuan et al. (Yuan, Burckel, Atanassov, & Fan, 2006; Yuan, Petsev, Prevo, Velev, & Atanassov, 2007). Nile Red powder was dissolved in ethanol to a concentration of 438 μM . 27.4 μL of this stock solution was then added to solutions of chitosan and butyl-modified chitosan, respectively, yielding final concentrations of 10 μM Nile Red in 20 μM solution of chitosan or butyl-modified chitosan. Chitosan scaffold films were made from these solutions by placing 30 μL of each solution onto a glass slide and then using a second glass slide to drag the meniscus at a rate of 1 $\mu\text{m/s}$ for ~30 min using an automated syringe pump (Cole-Parmer[®] Single-Syringe Infusion Pump, 74900). The entire process was executed in an enclosed chamber kept at 20 $^{\circ}\text{C}$ and greater than 95% humidity. Once the films were set, the slides were then frozen at $-20 \text{ }^{\circ}\text{C}$ for 1 h. There-

after the slides were vacuum freeze dried for 12 h. The resultant dried scaffold films were imaged using an Olympus Fluoview 1000 Laser Scanning Confocal Microscope. The fluorophores were excited at 515 nm. The resultant images were filtered using two band pass filters >650 and <620 nm, respectively.

3. Results and discussion

3.1. Free probe–polymer interaction

To explore the electrostatic nature of the chitosan probe interaction, we measured the steady state polarization of both positively charged probe, Rh123, and a negatively charged probe, fluorescein, in the presence of chitosan polymer. When the interaction of the fluorophore with the polymer is sufficient to retard its rotational motion, the measured polarization will increase relative to its value when freely suspended in buffer. Conversely, when there is an absence or minimal molecular interaction between the fluorophore and the polymer, the steady state fluorescent polarization will yield little to no change. As a relative control, we included a second negatively charged polymer (Eastman AQ55, Fig. 1C) as a compliment to the positively charged chitosan (Gennett & Purdy, 1990; Wang & Golden, 1989). Because Eastman AQ55 backbone is largely hydrophobic, whereas chitosan's is largely hydrophilic, its use also permitted both polar (i.e., charge–dipole and dipole–dipole) and non-polar (i.e., Van der Waals forces) interactions to be explored.

Table 1 presents the steady state fluorescent polarization of both Rh 123 and fluorescein in the presence and absence of chitosan polymer at pH 4.0 and 6.0. At these pH values, the Rh is positively charged, the fluorescein negatively charged, and the chitosan polymer positively charged at 4.0 but neutral to slightly positive at pH 6.0. Measurements at higher pH could not be considered because at values approaching and above the polymer's pKa (= 6.3) the polymer's side amine groups lose their protonation (i.e., positive charge) and the polymer precipitates out of solution. This is largely due to the fact that chitosan is actually a deacetylated derivative of chitin, a form of the polymer in which the amine groups are substituted with

highly hydrophobic acetylamine groups. Since commercial chitosan is roughly 80% deacetylated, 20% of the repeating monomer units retain the acetylamine groups of chitin, leaving the polymer insoluble unless the bulk of the free amine groups are protonated using dilute acetic acid.

In the case of Rh 123, the steady state fluorescence polarization did not change significantly upon addition of chitosan at a molar ratio of 30:1 at either pH. As both the probe and the polymer are either neutral or positively charged under these conditions, the absence of an increase in the steady state polarization suggests an absence of non-polar (i.e., hydrophobic) binding interactions between the fluorophore and the polymer. This is not a surprising result given the mostly hydrophilic nature of chitosan backbone. By contrast, the steady state fluorescent polarization of fluorescein increased significantly from 0.016 to 0.056 upon the addition of chitosan at a 30:1 molar ratio (pH 4, 20 mM). Increasing the pH to 6.0, which served to increase the negative charge on the fluorescein (Fig. 3), but also to decrease the degree of positive charge on the chitosan polymer, yielded similar results which also suggested electrostatic binding interaction between the positively charged polymer and slightly negative to neutrally charged fluorescein. Further evidence for this can be found in the titration binding curve performed at pH of 4 (Fig. 4A) wherein the polarization increased with increasing concentration of chitosan polymer.

To further verify that the dominant interaction between fluorescein and chitosan was electrostatic and not hydrophobic, a similar titration curve was executed in the presence of chitosan polymer after it had been modified to be more hydrophobic. The hydrophobically modified polymer, shown in Fig. 4B, had four carbon alkyl chains covalently bound to the free amine groups. Theoretically, if non-polar (i.e., hydrophobic) interactions contributed to the binding of fluorescein, a decrease in the concentration of modified chitosan polymer (relative to unmodified chitosan polymer) required in order to increase the polarization by 50% is expected. This data, shown in Fig. 4B, indicates the turning point for both the native and hydrophobically modified chitosan was comparable (~400:1), confirming that the dominant binding force was electrostatic. The fact that the rate of change (i.e., slope) was higher for the titration curve using hydrophobically modified chitosan likely indicates a distribution of binding affinities (i.e., there may be different probe–polymer interaction sites which have varying affinities, due to their microenvironments). The fact that the final measured polarization of the native chitosan is lower (than that for the modified chitosan) at the highest polymer level used indicates that complete saturation was not achieved. The relative strength of binding interaction between immobilization polymers can be observed by comparison against a different immobilization polymer. To do this we also titrated the positively charged Rh123

Table 1
Steady state fluorescent polarization – chitosan.

Polarization	Buffer (30 mM)		Chitosan:probe 30:1	
	pH 4	pH 6	pH 4	pH 6
Fluorescein	0.016 ± 0.002	0.020 ± 0.003	0.056 ± 0.005	0.060 ± 0.003
Rh 123	0.014 ± 0.001	0.015 ± 0.003	0.018 ± 0.002	0.016 ± 0.001

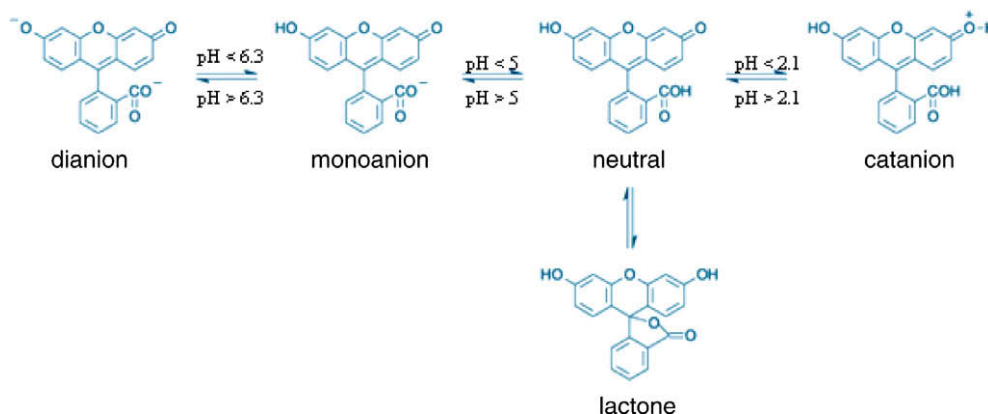


Fig. 3. Ionic forms of fluorescein as a function of pH.

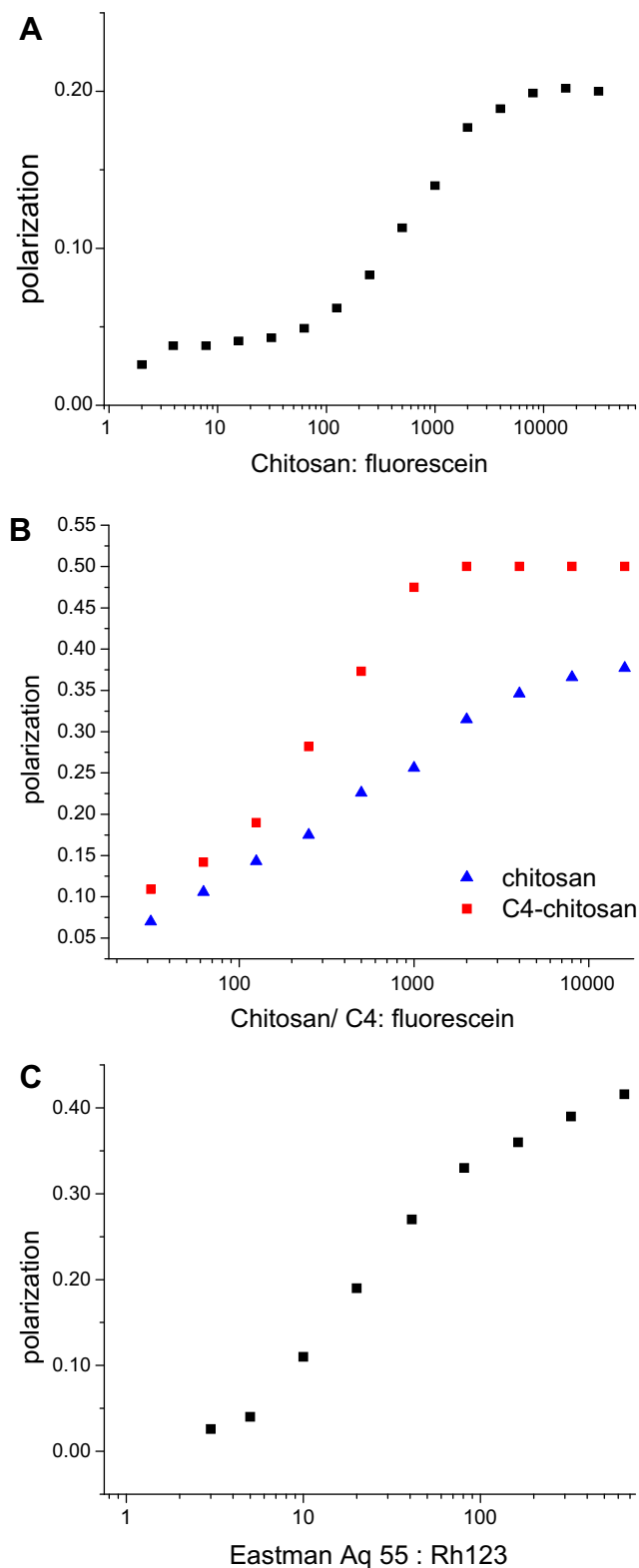


Fig. 4. Steady state fluorescent polarization binding curves of (A) fluorescein in chitosan (pH 4, 20 mM acetate buffer), (B) fluorescein in native and butyl-modified chitosan (pH 3.5, 20 mM acetate buffer), and (C) Rh123 in Eastman AQ55 (pH 8, 20 mM phosphate buffer).

with negatively charged Eastman AQ55 (Fig. 4C). In contrast to the fluorescein/chitosan system, a 50% increase in the polarization was achieved at a polymer to probe molar ratio of only 40:1, indicating much stronger binding in this system. In Table 2 we present steady

state polarization measurements. As expected, the positively charged RH123 interacted with the negatively charged Eastman AQ55 but did not with the negatively charged fluorescein.

3.2. Labeled enzyme–polymer interactions

In the previous sections steady state fluorescent polarization of freely suspended fluorophores was employed to probe the chemical microenvironment of polymers. It is also instructive to know how the polymer's micro-chemical environment impacts interaction with the enzyme. In a previous study it has been shown that the presence of a fluorophore attached to an enzyme does not significantly impact the interaction of the enzyme with the polymer (Konash et al., 2006). When investigating the rotational dynamics of an enzyme, however, the lifetime of the attached probe must be at least on the same order of magnitude as the rotational relaxation time of the enzyme to which it is attached. In other words, the choice of the probe is governed by the size of the enzyme. The enzyme used in this work, alcohol dehydrogenase (YADH, MW = 144 kDa), possesses a theoretical rotational relaxation time on the order of $\rho \sim 180$ ns (assuming a rigid spherical model). We selected the fluorophore 2,5-dansyl chloride because possesses stability, charge neutrality, and suitable lifetime of ~ 28 ns.

In order to mimic the pH conditions in the chitosan solutions, the steady state fluorescent polarization ($P = 0.23$) of 2,5-dansyl chloride attached to YADH was measured in an acetate buffer (20 mM, pH 3.5). When the labeled enzyme was placed in the presence of unmodified and modified chitosan, the steady state fluorescent polarization increased only slightly for both polymers (from $P = 0.25$ to $P = 0.26$, respectively). At first glance this would suggest that the interaction between the enzyme and the polymer was relatively minor and unaffected by any impact of the hydrophobic modification upon the resultant micellar structure. When analyzing the emission of fluorophores attached to enzymes, however, there are two contributions to the steady state fluorescence polarization that must be considered: (1) the local rotation of the fluorophore about its point of attachment and (2) the global rotational motion of the enzyme. The distinction between the two is required because the contribution to the steady state polarization from the local motion of the fluorophore (i.e., about its axis of rotation) may not be affected by the binding capacity (i.e., chemical microenvironment) of the polymer. As such, to use steady state fluorescent polarization measurements to compare the relative binding capacity of different polymers to labeled enzymes, the contributions made from each rotational component must be resolved using time-resolved fluorescence techniques (Jameson & Hazzlett, 1991).

Time-resolved fluorescence measures the lifetime components of the system, and thus the contribution of different rotational modes to the steady state polarization. The results, presented in Table 3, suggest that the lifetime components of the probe–enzyme system in acetate buffer are complex and best characterized by three exponentials. For each polymer system the measured lifetimes (i.e., long and short components) were relatively unchanged from their values in free solution, indicating that the quantum yield of the dansyl moiety was unaffected by the polymer matrix. Next, the rotational relaxation modes of the labeled enzyme in the absence and presence of polymer were determined. The results indicated a complex rotational scheme best characterized by three rotational relaxation modes: one slow ($\rho = 90$ ns) and two faster contributions ($\rho = 5$ ns and 0.21 ns) for enzyme in buffer alone. The slow rotational relaxation time of 90 ns is consistent with global rotation of a large protein. The fact that it is less than the 180 ns calculated for a rigid spherical protein is most likely due to domain movement in the protein which has been found for most protein systems (see for example, Hamman, Oleinikov, Jokhadze, Traut, & Jame-

Table 2
Steady state fluorescent polarization – Eastman AQ55.

	Phosphate buffer (30 mM)			Eastman AQ 55:probe (30:1)		
	pH 6	pH 8	pH 10	pH 6	pH 8	pH 10
Fluorescein	0.020 ± 0.003	0.025 ± 0.002	0.025 ± 0.001	0.020 ± 0.003	0.018 ± 0.002	0.019 ± 0.002
Rh 123	0.015 ± 0.003	0.018 ± 0.003	0.016 ± 0.003	0.248 ± 0.004	0.232 ± 0.002	0.231 ± 0.003

Table 3
Lifetime and rotational relaxation time for dansyl-chloride labeled yeast alcohol dehydrogenase (DNS-YADH).

	$P(\pm 0.002)$	τ_1	τ_2	τ_3	ρ_1	ρ_2	ρ_3
DNS-YADH in buffer	0.23	27.3	1.0	5.9	90	5	0.21
DNS-YADH in chitosan	0.25	27.9	0.8	5.5	115	6.9	0.23
DNS-YADH in C4-chitosan	0.26	27.7	0.9	5.3	95	7.6	0.39

son, 1996). When the labeled enzyme was placed in the unmodified and butyl-modified chitosan, there were no significant changes in the recovered rotational relaxation time (see Table 3). This observation suggests that no significant interaction between the polymer and the enzyme existed, and that the slight increase in steady state polarization observed may, in fact, be due to a small increase in the bulk solvent viscosity due to the polymer.

3.3. Characterization of hydrophobically modified polymer

Since many fluorophores are hydrophilic and since in this case the dominant contribution to steady state fluorescent polarization is electrostatic, an alternative method to detect the relative presence of polar and non-polar regions was applied. This method involves using fluorophores whose emission spectra are sensitive to the polarity of their immediate microenvironment. In this regard, the hydrophobically modified chitosan was further characterized using the fluorophore 1,8-anilinonaphthalene (ANS). The unusual environment sensitivity of 1,8-ANS was first reported in 1954 by Weber and Laurence (1954). While weak in aqueous solution, the fluorescence of 1,8-ANS markedly increases in less polar environments (Azari, Hosseinkhani, & Nemat-Gorgani, 2001; Semisotnov et al., 1991). It has also been shown that a shift of the fluo-

rescence emission peak from ~520 to ~475 nm occurs as the polarity of the probe's immediate microenvironment decreases (Lee, Chen, & Chang, 1988). This characteristic has been widely used in the study of both protein denaturation and membrane characterization (Dautzenberg, Burkart, Rother, Schellenberger, & Mansfeld, 1991; Gabellieri & Strambini, 2006; Matulis, Baumann, Bloomfield, & Lovrien, 1999; Semisotnov et al., 1991; Slavik, 1982; Tan & Belanger, 2005; Wilkinson-White & Easterbrook-Smith, 2007). In this work, ANS has been used to characterize the extent to which chemical addition of alkyl chains of varying length enhanced the hydrophobicity of the chitosan polymer.

Assuming a relatively consistent degree of amine substitutions along the chitosan backbone, one should expect an increase in the quantum yield and a blue shift in the ANS emission that correlates with the increased length of the hydrophobic side chains, (i.e., ANS in octyl-modified chitosan should have a higher quantum yield and greater blue-shifted emission when compared against butyl-modified chitosan). With respect to controls, there should be significantly less fluorescence associated with ANS when in the presence of acetic acid or the unmodified chitosan, as both solutions are not expected to provide the type of non-polar environments that will alter the fluorescence properties of ANS. The results are presented in Fig. 5. As expected, there was no measurable shift associated with addition of ANS to 40 μ M chitosan dissolved in acetic acid (0.2 M), suggesting that these two systems provide predominantly hydrophilic chemical microenvironments. However, when added to equal concentrations (40 μ M) of butyl- and octyl- modified chitosan, the emission intensity of ANS increased and demonstrated a blue shift, confirming the presence

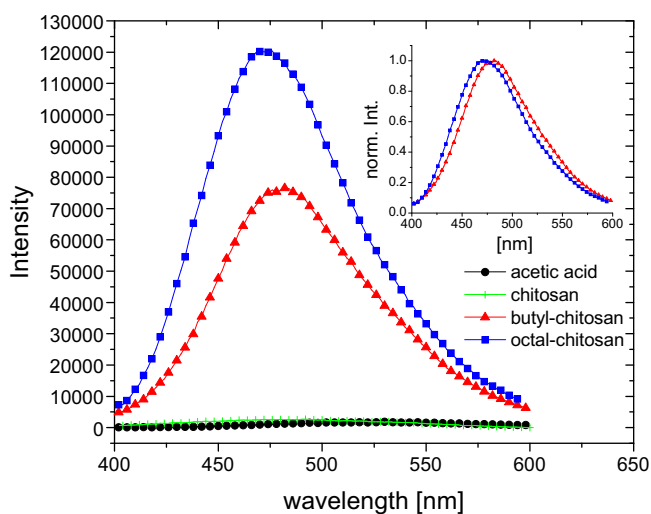


Fig. 5. (a) intensity as a function of wavelength for ANS in 0.2 M acetic acid, unmodified chitosan, butyl- and octyl-modified chitosan (b) normalized intensity of butyl- and octal-modified chitosan, indicating a wavelength shift ~10nm.

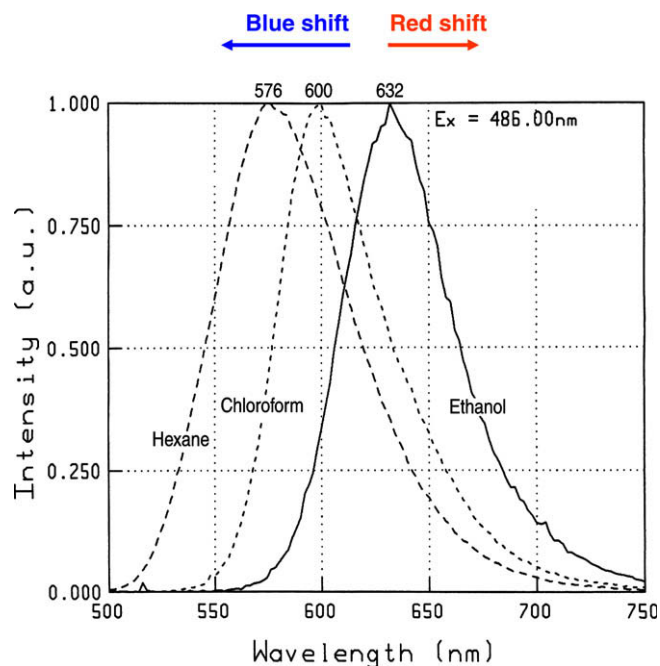


Fig. 6. Normalized emission profile of Nile Red in solvents of varying polarity. Dielectric constants were 1.89 for hexane (at 20 °C), 4.8 for chloroform (at 20 °C) and 24.3 for ethanol (at 25 °C). (From Elsey, Jameson, Raleigh & Cooney, 2007).

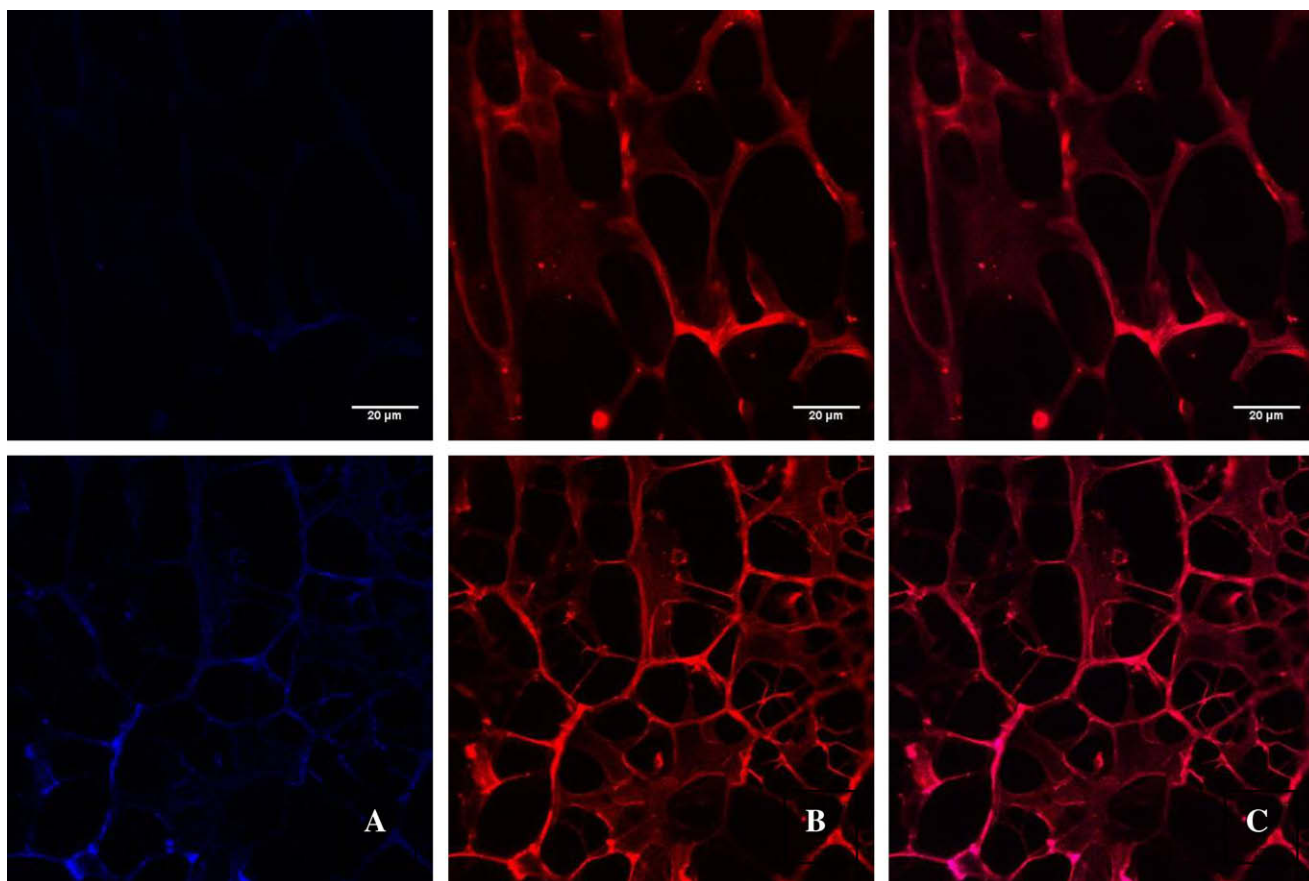


Fig. 7. Laser scanning confocal microscopy images of chitosan scaffolds incorporating Nile Red fluorophore. (For interpretation of color mentioned in this figure the reader is referred to the web version of the article.)

of non-polar chemical microenvironments. The insert illustrates a shift in the peak intensity of ~ 10 nm, between butyl and octyl-modified chitosan, further confirming that the modification did increase the relative hydrophobic chemical microenvironment of the chitosan modified with the longer alkyl chain length.

It has been proposed that the hydrophobically modified chitosan described above theoretically forms amphiphilic micelles on the mesopore scale. These micelles become more hydrophobic due to the introduction of the hydrophobic side alkyl chains along an otherwise hydrophilic backbone (Klotzbach et al., 2006, 2008).

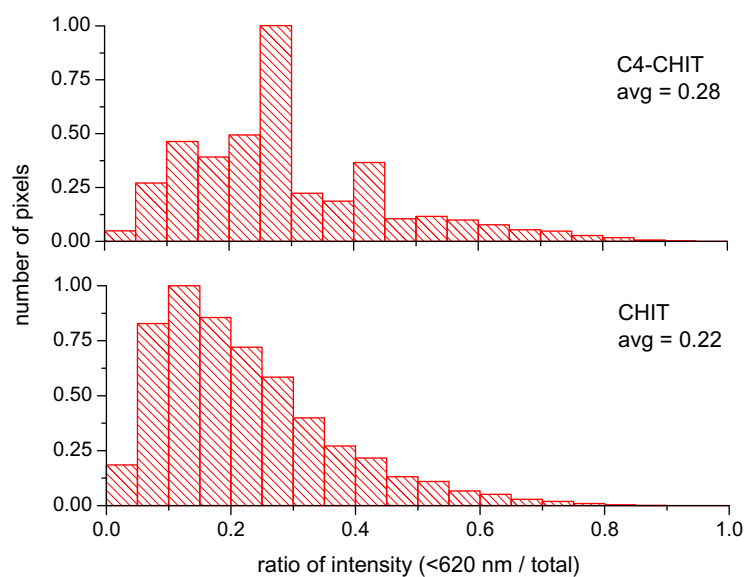


Fig. 8. Ratio of the blue region intensity to the total emission intensity for modified and unmodified chitosan. (For interpretation of color mentioned in this figure, the reader is referred to the web version of this article.)

To test this theory, scaffolds were fabricated from solutions of unmodified and modified chitosan that also contained Nile Red, a fluorophore whose emission profile changes in both intensity and maximum in response to changes in the polarity of the surrounding solvent (Fig. 6) (Else, Jameson, Raleigh, & Cooney, 2007). Laser scanning confocal microscopy was used to image slices of the scaffolds, using filters that permitted light above 650 nm (red region) and below (blue region) 620 nm (Fig. 7) to be detected. In Fig. 7, the top row of images presents the emission below 620 nm (A), above 650 nm (B), and their combined emission (C) for scaffolds fabricated from the unmodified chitosan. The bottom row of images presents the emission below 620 nm (A), above 650 nm (B), and their combined image (C) for scaffolds fabricated from the modified chitosan. Fig. 8 presents the distribution for the ratio of the emission intensity below 620 nm to the total emission intensity. The increase in the average from the unmodified, to modified chitosan (C4-chitosan) indicates an increase in the hydrophobic nature of the polymer.

4. Conclusions

The use of polar sensitive fluorophores in combination with fluorescent spectroscopy and microscopy provides a unique and informative tool for probing the chemical microenvironment provided by immobilization polymers. In this work, these techniques were used to probe the chemical microenvironments of native and hydrophobically modified chitosan polymer matrices used to immobilize enzymes. Our results indicate that electrostatic forces dominate the interaction between fluorophores and polymer when both are freely suspended in solution. Also, at least in the case of yeast alcohol dehydrogenase labeled with dansyl-chloride, there is no significant change in the local or global motion of the enzyme-bound fluorophore when placed in the presence of either unmodified or butyl-modified chitosan. This suggests that the immobilization of enzyme into chitosan amphiphilic micelles does not occur in the aqueous phase, as described by Klotzbach et al. (2006), but more likely during the scaffold formation step. Introducing side alkyl chains of increasing carbon length (along the chitosan polymer backbone) results in a modified chitosan polymer that is more hydrophobic and amphiphilic. Future work will include the application of pH sensitive fluorophores and correlation of the polymer's amphiphilic nature to enzyme activity and stability.

Acknowledgements

The authors gratefully acknowledge support from the Office of Naval Research (contract number N0014-01-1-0928) through the Hawaii Environmental and Energy Technology (HEET) initiative (Richard Rocheleau, PI), and from the AFOSR Multidisciplinary University Research Initiative program (award number FA9550-06-1-0264) under the Fundamentals and Bioengineering of Enzymatic Fuel Cells award (P. Atanassov, PI). The authors also thank Plamen Atanassov and Rosalba Rincon for help in transferring the film fabrication technique from their lab to ours, and Carolin Lau for fabrication of the hydrophobically modified chitosan.

References

Azari, F., Hosseinkhani, S., & Nemat-Gorgani, M. (2001). Use of reversible denaturation for adsorptive immobilization of urease. *Applied Biochemistry and Biotechnology*, 94, 265–277.

- Cooney, M. J., Petermann, J., Lau, C., & Minteer, S. D. (2009). Characterization and evaluation of hydrophobically modified chitosan scaffolds: Towards design of enzyme immobilized flow-through electrodes. *Carbohydrate Polymers*, 75(3), 428–435.
- Dautzenberg, H., Burkart, J. K., Rother, P. G., Schellenberger, A., & Mansfeld, J. (1991). Interaction of invertase with polyelectrolytes. *Biotechnology and Bioengineering*, 38(9), 1012–1019.
- Gratton, E. (2006). *Globals for Spectroscopy*. In E. Gratton (Ed.), *Globals*. Irvine: Globals Software.
- Else, D., Jameson, D. M., Raleigh, B., & Cooney, M. J. (2007). Fluorescent measurement of microalgal neutral lipids. *Journal of Microbiological Methods*, 68(3), 639–642.
- Gabellieri, E., & Strambini, G. B. (2006). ANS fluorescence detects widespread perturbations of protein tertiary structure in ice. *Biophysical Journal*, 90(9), 3239–3245.
- Gennett, T., & Purdy, W. C. (1990). Voltammetric determination of the ion-exchange behavior of AQ polymers [poly(ester sulfonic acid) anionomers] in acetonitrile. *Analytical Chemistry*, 62(19), 2155–2158.
- Hamman, B. D., Oleinikov, A. V., Jokhadze, G. G., Traut, R. R., & Jameson, D. M. (1996). Dimer/monomer equilibrium and domain separations of *Escherichia coli* ribosomal protein L7/L12. *Biochemistry*, 35(51), 16680–16686.
- Jameson, D. M., & Hazzlett, T. L. (1991). Time-resolved fluorescence in biology and biochemistry. In T. G. Dewey (Ed.), *Biophysical and biochemical aspects of fluorescence spectroscopy* (pp. 105–133). New York: Plenum Publishing Corp.
- Klotzbach, T., Watt, M., Ansari, Y., & Minteer, S. D. (2006). Effects of hydrophobic modification of chitosan and Nafion on transport properties, ion-exchange capacities, and enzyme immobilization. *Journal of Membrane Science*, 282(1–2), 276–283.
- Klotzbach, T. L., Watt, M., Ansari, Y., & Minteer, S. D. (2008). Improving the microenvironment for enzyme immobilization at electrodes by hydrophobically modifying chitosan and Nafion® polymers. *Journal of Membrane Science*, 311(1–2), 81–88.
- Konash, A., Cooney, M. J., Liaw, B. Y., & Jameson, D. M. (2006). Characterization of enzyme-polymer interaction using fluorescence. *Journal of Materials Chemistry*, 16, 4107–4109.
- Krajewska, B. (2004). Application of chitin- and chitosan-based materials for enzyme immobilizations: A review. *Enzyme and Microbial Technology*, 35(2–3), 126–139.
- Lee, H.-J., Chen, Y.-H., & Chang, G.-G. (1988). Fluorescence studies on the dissociation and denaturation of pigeon liver malic enzyme. *Biochimica et Biophysica Acta (BBA) – Protein Structure and Molecular Enzymology*, 955(2), 119–127.
- Martin, G. L., Minteer, S. D., & Cooney, M. J. (2009). Spatial distribution of malate dehydrogenase in amphiphilic chitosan scaffolds. *ACS Applied Materials & Interfaces*, 1(2), 367–372.
- Matulis, D., Baumann, C. G., Bloomfield, V. A., & Lovrien, R. E. (1999). 1-Anilino-8-naphthalene sulfonate as a protein conformational tightening agent. *Biopolymers*, 49(6), 451–458.
- Perrin, F. (1925a). Theorie de la fluorescence polarisee (influence de la viscoite). *Comptes Rendue*, 180, 581–583.
- Perrin, F. (1925b). Sur le mouvement brownien de rotation. *Comptes Rendue*, 181, 514.
- Perrin, F. (1926). Polarisation de Lumiere de Fluorescence. *Journal de Physique*, 7, 390–401.
- Semisotnov, G. V., Rodionova, N. A., Razgulyaev, O. I., Uversky, V. N., Gripas, A. F., & Glimanshin, R. I. (1991). Study of the “molten globule” intermediate state in protein folding by a hydrophobic fluorescent probe. *Biopolymers*, 31, 119–128.
- Slavik, J. (1982). Anilinonaphthalene sulfonate as a probe of membrane composition and function. *Biochimica et Biophysica Acta (BBA) – Reviews on Biomembranes*, 694(1), 1–25.
- Tan, S., & Belanger, D. (2005). Characterization and transport properties of Nafion/polyaniline composite membranes. *Journal of Physical Chemistry B*, 109(49), 23480–23490.
- Wang, J., & Golden, T. (1989). Permselectivity and ion-exchange properties of Eastman-AQ polymers on glassy carbon electrodes. *Analytical Chemistry*, 61(13), 1397–1400.
- Weber, G. (1952a). Polarization of the fluorescence of macromolecules. *Biochemistry Journal*, 51, 145–155.
- Weber, G. (1952b). Polarization of the fluorescence of macromolecules. 2. Fluorescent conjugates of ovalbumin and bovine serum albumin. *Biochemistry Journal*, 51(2), 155–167.
- Weber, G., & Laurence, D. J. R. (1954). Fluorescent indicators of adsorption in aqueous solution and on the solid phase. *Biochemical Journal*, 56, xxxvi.
- Wilkinson-White, L. E., & Easterbrook-Smith, S. B. (2007). Characterization of the binding of Cu(II) and Zn(II) to transthyretin: Effects on amyloid formation. *Biochemistry*, 46(31), 9123–9132.
- Yuan, Z., Burckel, D. B., Atanassov, P., & Fan, H. (2006). Convective self-assembly to deposit supported ultra-thin mesoporous silica films. *Journal of Materials Chemistry*, 16, 4637–4641.
- Yuan, Z., Petsev, D. N., Prevo, B. G., Veleev, O. D., & Atanassov, P. (2007). Two-dimensional nanoparticle arrays derived from ferritin monolayers. *Langmuir*, 23(10), 5498–5504.